Chapter 6

Electric Field Induced Tuning of Molecular Conformation to Acquire Spintronics Property in Biphenyl Systems

In this chapter we have theoretically studied the effect of external electric field on biphenyl, methylene substituted biphenyl monoradical and diradical systems. It has been found that the molecular conformation changes with application of external electric field. Thus, it is possible to tune molecular conformation reversibly only by external electrical stimuli. The HOMO-LUMO gap of the diradical reduces under external electric field. The molecules with low HOMO-LUMO gap can be used as unimolecular rectifier if the HOMO and LUMO have different spatial location on the molecule. Either to be conductive, the molecule should have the HOMO and LUMO located on the same spatial position. It has been observed that the diradical can be used as both unimolecular rectifier and molecular conductor depending upon the field strength. Now, the insulator molecule can be switched to molecular rectifier or molecular conductor and vice versa by external electric field. The spin topology in a radical depends on the strength and direction of the applied electric field. Consequently the extent of magnetic coupling in diradical system changes with external electric field. We have calculated the transmission spectra and I-V curve for the diradical at different dihedral angles. At lower dihedral angle the diradical shows efficient spin filter behavior. It is now possible to use a single molecule for multifarious application like unimolecular rectifier, spin filter and molecular conductor depending upon the strength of the applied electric field.

6.1 Introduction

Different isomers of a molecule can have different optical and electronic properties. Their conformational flexibility can also give rise to interesting transport properties, and a simple manipulation of their composition and geometry can lead to a wide variety of binding, optical and structural properties, which can be efficiently tuned according to specific need.[1,2] A small change in conformational angle can lead to a wide change in the current-voltage (*I-V*) characteristics of a molecular device.[3] The physiological properties of molecules are also dependent on dihedral angle. As for example, physiological property and lipid solubility of poly chlorinated biphenyl is dependent on its degree of planarity. The degree of planarity can be controlled by the position of substitution.[4] To get a desired conformation by chemical substitution we must compromise with its chemical constitution. However, an applied electric field to a molecule reorganizes the electronic distribution and changes the Hellmann-Feynman force acting on the constituent nuclei without altering the chemical constitution. The field also exerts a force directly on the nuclei. The resulting net force will cause a change in molecular geometry and vibrational force constant.[5,6] The effect of uniform static electric field on some aliphatic and aromatic compounds is studied within the density functional theory framework by Rai et al.[7] They found that the electric field perturbs the molecular geometry and shifts the infrared (IR) vibrational frequencies accompanied by spectral intensity redistribution. It has also been found that the energy gap between highest occupied molecular orbital (HOMO) and lowest unoccupied molecular orbital (LUMO) is diminished rapidly when the LUMO possesses predominant π-character. It has also been shown that the geometric and electronic structure of conjugated molecular wire is very sensitive to the external electric field. The increasing field strength leads to higher conjugation in conjugated molecular wire.[8]

The external electric field leads to spatial redistribution of frontier molecular orbitals. Electrical conduction through molecules essentially requires "promoting" an electron to erstwhile virtual, unoccupied molecular orbitals (UMOs).[7] The contribution of higher UMOs and lower occupied MOs to the current conduction through molecule has been investigated by Wang et al.[9] It has been found that the upper UMOs contribute significantly to the electron conduction than the low lying ones.[10] Organic radicals show fascinating transport properties such as

spintronic behavior like spin filter,[11] spin current conduction[12] etc. Because of their weak spin-orbit and hyperfine interactions, organic molecules are attractive for such components.[13]

The biphenyl molecule is planar or nearly so in the solid state[14-16] and twisted to about 40° around the central C-C single bond in the vapor phase.[17] The energetics of the internal rotation around C-C single bond between two benzene rings is difficult to interpret.[18] Bastiansen and Samdal experimentally estimated the rotational barrier to be 6.0 ± 2.1 kJ/mol and 6.5 ± 2.0 kJ/mol for 0° and 90° dihedral angles respectively.[19] Mono nitronyl-nitroxide substituted biphenyls are synthesized by Stroh et al.,[20] and they found that the dihedral angle between two benzene rings vary for ortho and meta substitutions. Recently, biphenyl coupled diradical has been synthesized and it is found that the dihedral angle between two phenyl rings is less than 1° in the crystalline state, whereas DFT optimized structure shows the angle is 35°.[21]

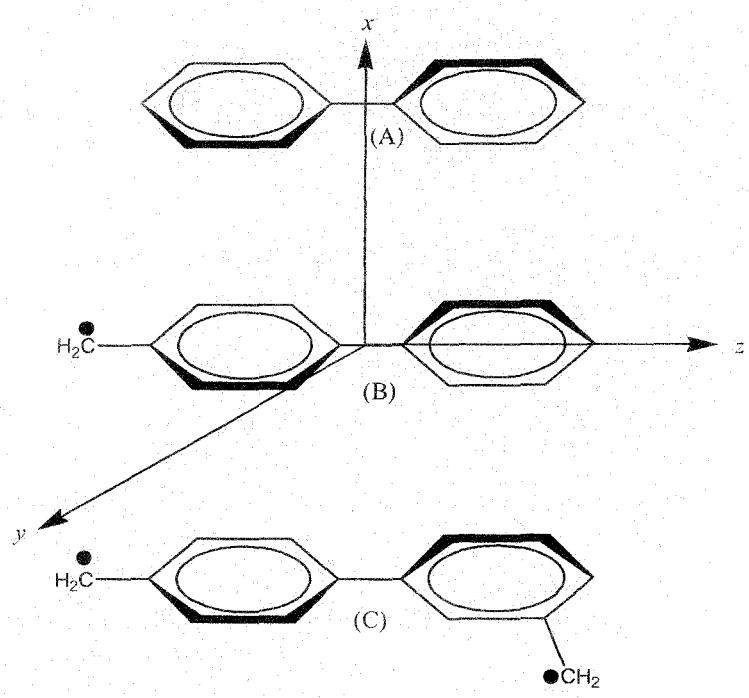

Figure 6.1 Molecules and radicals under investigation (A) biphenyl (B) methylene substituted biphenyl monoradical and (C) methylene substituted biphenyl diradical. The *z* axis is parallel to molecular plane and *x* axis is perpendicular to the molecular plane.

The spirit underlying in this work is to understand the response of molecules and radicals under external electric field. In this study we choose biphenyl, methylene substituted biphenyl monoradical and diradical systems (Figure 6.1). We apply electric field parallel to the molecule ($E_{\parallel}$) and perpendicular to the diagonal plane of two phenyl rings ($E_{\perp}$). Possible application of external electric field effect on molecule and radicals have been studied. Investigations on the change of shape and energy of molecular orbitals, spin density distribution and magnetic properties of the radicals under electric field have also been done. We have studied the spin filtering ability of the diradical at different conformations to understand the spintronics behavior. The current voltage (*I-V*) curve has also been presented to elucidate the conductivity of the diradical at different dihedral angles.

6.2 Results and Discussions

6.2.1 Effect of external electric field on molecular geometry

We have optimized all the geometries in the unrestricted DFT framework using B3LYP functional and 6-31+G (d,p) basis set. All the calculations have been done using Gaussian09W[22] package unless otherwise mentioned. In absence of an external electric field, geometry optimization of biphenyl results stable non-planar conformation. Biphenyls have different dihedral angles depending on their phases. It is known to have 0° dihedral angle in solid phase, around 40° in the vapor phase and in between in the solution phase.[23] The dihedral angle can be changed by substitution for desired application. It is already reported that the conjugation length,[24] or the delocalization of electrons,[25] depends strongly on the molecular conformation and most importantly on the joint alignment of adjacent aromatic rings. It is also suggested that molecular conductivity reaches the maximum value when neighboring aromatic ring adopts a coplanar arrangement.[26] To get a desired conformation of molecule for various application we employ external electric field. Starting from 40.40° dihedral angle if we apply $E_{\parallel}$, the dihedral angle gradually decreases with increase in the applied field strength (Table 6.1). In case of $E_{\perp}$, we are able to optimize the structure up to 0.003 a.u. field strength.

Table 6.1 Dihedral angles of Biphenyl, Monoradical and Diradical under External Electric Eield (1 a.u. field strength = 51.42 V/Å)

Field Strength $\times 10^{-4}$ a.u.	Dihedral Angle (°)					
	Biphenyl		Monoradical		Diradical	
	$E_{\parallel}$	$E_{\perp}$	$E_{\parallel}$	$E_{\perp}$	$E_{\parallel}$	$E_{\perp}$
0	40.40	40.40	35.12	35.12	33.32	33.32
15	40.34	39.82	35.03	35.16	33.20	33.43
30	40.13	41.06	34.62	35.29	32.75	33.60
45	39.75	-------	33.97	35.50	32.04	33.94
60	39.26	-------	32.85	35.81	31.03	34.28
75	38.66	-------	31.91	36.21	29.79	34.90
90	37.91	-------	30.45	36.72	28.34	35.52
115	------	------	27.45	37.81	26.59	------
130	------	------	27.45	38.59	23.20	------
145	------	------	27.45	39.58	21.10	------
160	------	------	27.45	40.76	35.70	------
Max. Change	2.49	0.66	7.67	5.55	12.22	2.2

When we optimize the methylene substituted biphenyl mono-radical we get non-planar geometry with dihedral angle ~35°. Stroh et al.[20] synthesized ortho nitronyl-nitroxide radical substituted biphenyl and they found that the dihedral angle between two phenyl rings is 46.3° in the solid state. Whereas, in case of meta substitution they found two structures with dihedral angles 25.9° and 19.5° respectively in the solid state. For $E_{\parallel}$ the dihedral angle gradually decreases. On the other hand, in case of $E_{\perp}$ the dihedral angle increases with the increasing field strength (Table 6.1).

The optimized geometry of methylene substituted biphenyl diradical is found to be non-planar. Mostovich et al.[21] isolated the nitronyl-nitroxide substituted biphenyl diradical where the coupler biphenyl is planar in the solid state. When we apply $E_{\parallel}$ on non-planar structure of the

diradical the dihedral angle decreases. On the other hand, if one applies the field $E_{\perp}$, the dihedral angle increases with increasing field strength (Table 6.1).

So far from the above discussion we have seen that molecular conformation changes reversibly under external electric field. This result is very impressive because one can tune the molecular conformation according to the need only by external stimuli without any chemical substitution. A small change in molecular conformation leads to the change in electronic structure, transport property, energy of MO, and spatial distribution of MO. These changes are systematically discussed in the upcoming sections of this manuscript.

6.2.2 Molecular orbital analysis

The energy and spatial distribution of molecular orbitals are function of molecular conformation and external electric field.[27] Therefore, it is important to analyze the molecular

Table 6.2 HOMO-LUMO Gap of the Molecules under Different Electric Field ($E_{\parallel}$) (1 a.u. field strength = 51.42 V/Å)

Field×10−4 a.u. ($E_{\parallel}$)	HOMO-LUMO Gap (eV)		
	Biphenyl	Monoradical	Diradical
0	5.27	4.22	4.17
15	5.26	4.02	4.03
30	5.21	4.56	3.86
45	5.13	4.42	3.67
60	5.02	4.31	3.48
75	5.22	4.09	3.00
90	4.47	2.64	2.51
115	---	4.04	1.74
130	---	2.57	0.95
145	---	2.18	0.35
160	---	1.80	0.34

orbitals for different conformations and under external electric field to understand the molecular behavior. The molecular orbitals are important to understand the transport property through a molecule because they contain all the quantum mechanical information about molecular electronic structures and offer spatial conduction channels for electron transport.[28] Therefore, the modulation of the MOs, i.e., the localization of orbitals can significantly change the transport properties. External electric field is an appropriate stimulus to tune the MOs of a molecule. It has

been shown that the MOs of a molecule with and without electrode atoms in their end have similar characteristics under external electric field.[29] Following this analogy, we apply electric field without lead atoms to study the change of molecular orbitals and their energy spectrum in case of biphenyl, methylene substituted biphenyl monoradical and diradical under external electric field.

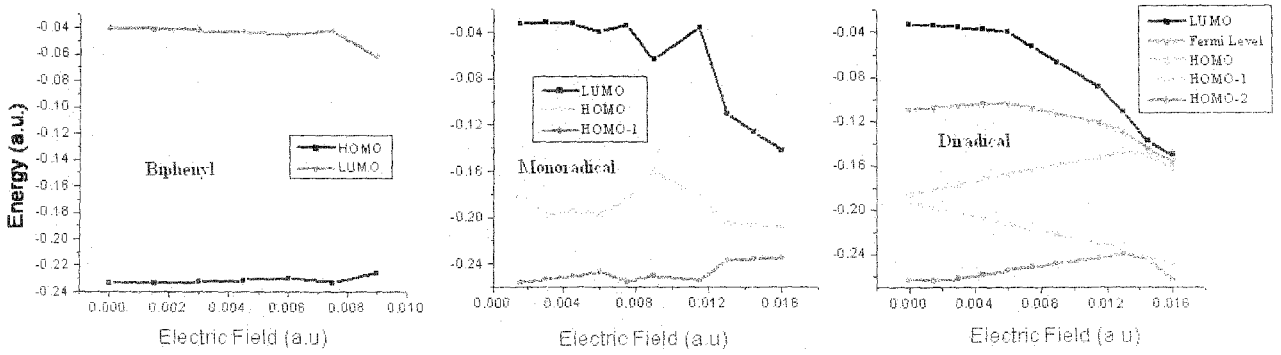

Figure 6.2 Energy ordering of molecular orbital of biphenyl, monoradical and diradical.

The highest occupied and lowest unoccupied molecular orbitals play a crucial role in the transport properties of molecules.[30] The Fermi level lies in between the HOMO and LUMO energies of the molecule. When the LUMO is aligned with the Fermi level; electrons begin to tunnel through the molecule. The HOMO-LUMO (HL) gap (Table 6.2) of biphenyl gradually decreases with increasing field strength; i.e., the LUMO tends to go near the Fermi level (Figure 6.2). In case of biphenyl system, we are able to optimize the geometry up to the field strength 0.009 a.u. This may be due to the imbalance between the total force generated from the net charge and the external electric field.[31]

With the change in dihedral angle, the shape of molecular orbital also changes.[3] Here, we found that at field strength 0.0075 a.u. and beyond the shape of molecular orbital is drastically changed. From Figure 6.3 it is clear that at higher field strength the spatial distribution of MOs (HOMO and LUMO) are different; i.e., the location of the MOs are different. It is known that if the location of HOMO and LUMO is different and the HOMO-LUMO energy gap is significantly low (~0.3 eV) the molecule can act as an unimolecular rectifier.[3,32] Therefore, one can say that biphenyl can act as unimolecular rectifier if the HOMO-LUMO gap reduces further.

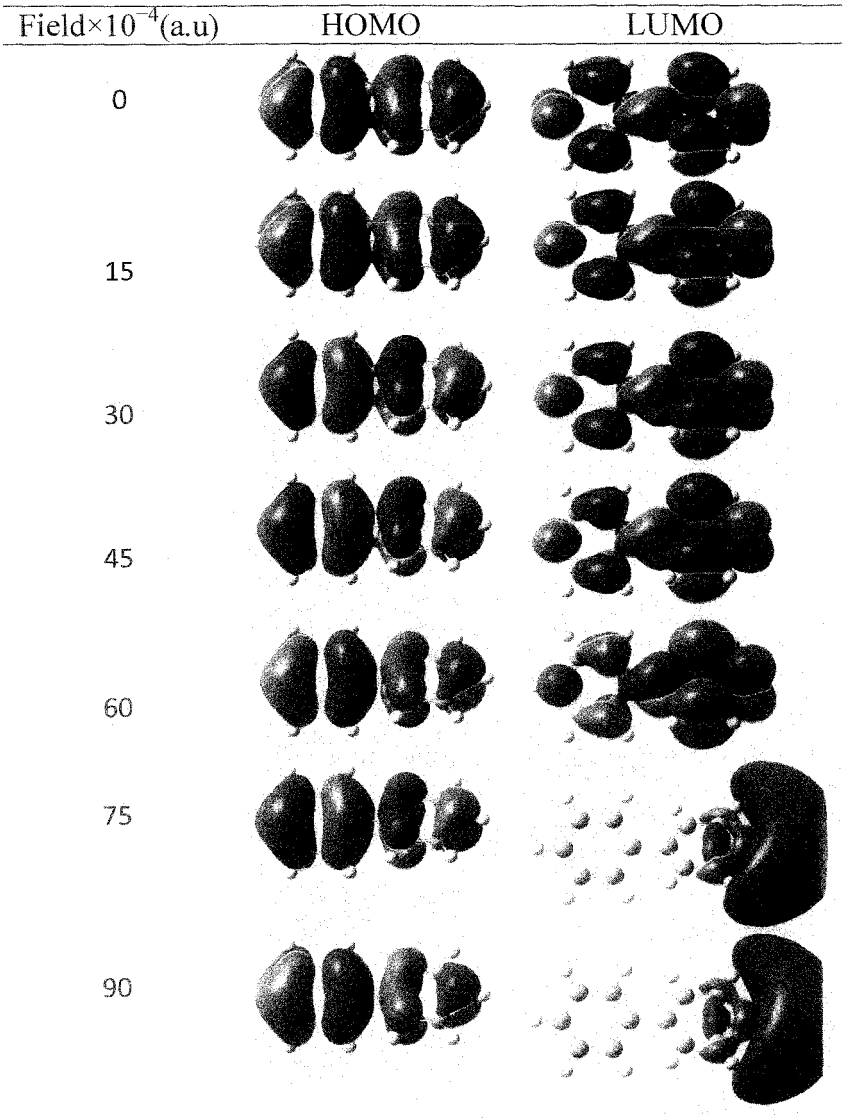

Figure 6.3 The molecular orbital picture of biphenyl at various field strength ($E_{\parallel}$).

The energy of MOs of the monoradical randomly changes with $E_{\parallel}$(Figure 6.2). With increasing field strength the energy gap between HOMO and LUMO decreases. Here, the HOMO is actually a singly occupied MO (SOMO). However, for $E_{\perp}$, energy of MOs remains unaltered. Another point is that with increasing field strength HOMO-1 and LUMO are localized, whereas HOMO is delocalized (Figure 6.4). As the HOMO and LUMO lies near the Fermi level, it is possible to tunnel the unpaired electron from HOMO to the LUMO easily. On the other hand HOMO and LUMO have different spatial position which is prerequisite for a molecule to be a unimolecular rectifier.[32] Therefore, the monoradical will conduct the spin

current as the transport occurs mainly through LUMO[3] and stable organic monoradicals can be used as efficient unimolecular rectifier.

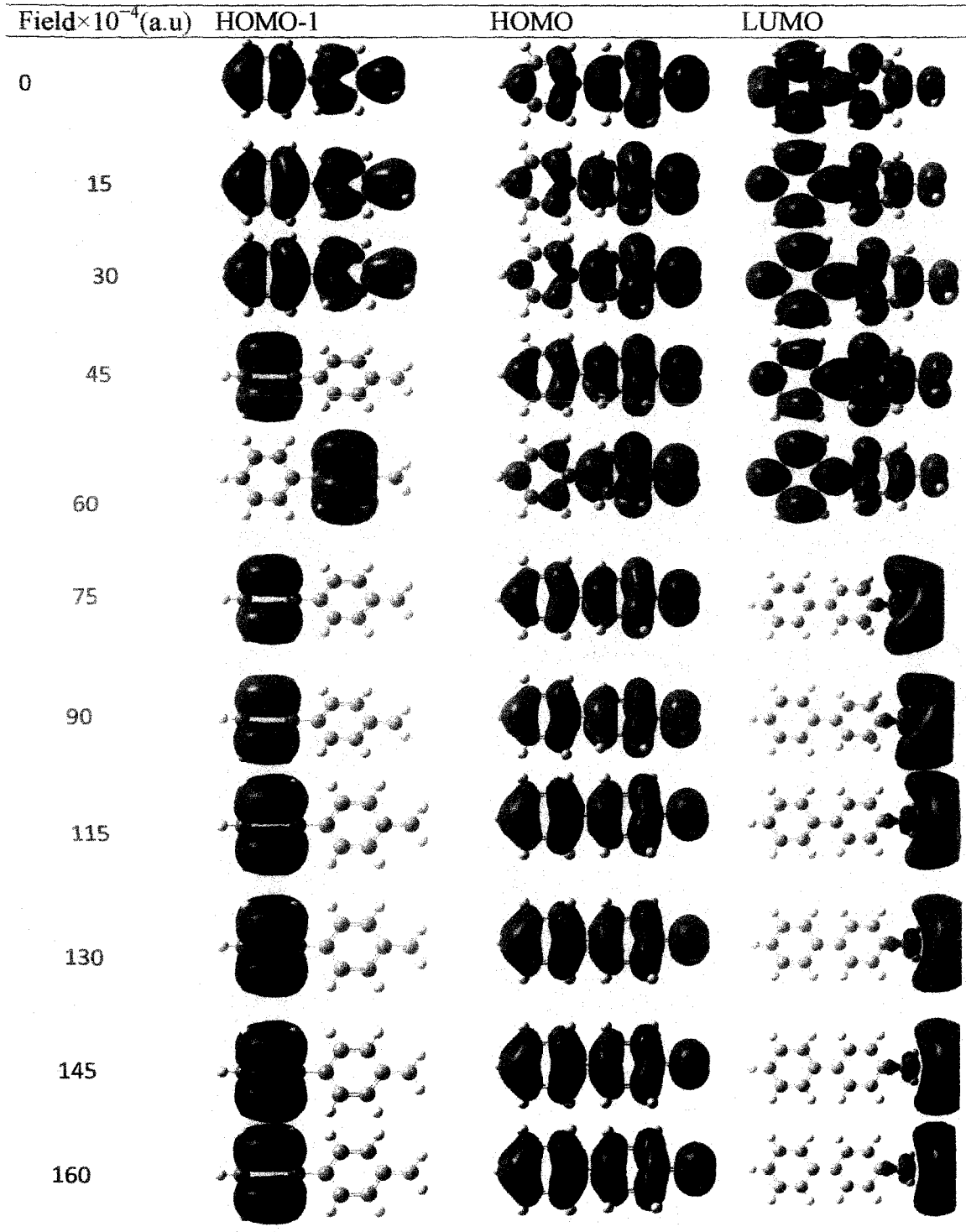

Figure 6.4 The molecular orbital picture of monoradical at various field strength($E_{\parallel}$).

In case of diradical the LUMO, HOMO-1 and HOMO-2 are mostly affected by external electric field. Here, HOMO and HOMO-1 are actually two SOMO's. It is clear from Figure 6.2 that the energy of LUMO and HOMO-1 reduces and energy of HOMO increases with rising field strength ($E_{\parallel}$). It is now obvious that for $E_{\parallel}$, with growing field strength LUMO and HOMO lie near the Fermi level (Figure 6.2); i.e., one can say electron can tunnel from the HOMO (SOMO) to LUMO. The HL gap narrows significantly between 0.0075-0.0145 a.u. field strength. The HL gap is a function of conformation and external electric field.[27] Not only the energy of MO but also the spatial distribution of MOs over the molecule is the function of conformation and external electric field. We can see from Figure 6.3, Figure 6.4, and Figure 6.5 that beyond the field strength of 0.0075 a.u. the LUMO is localized over few atoms. Therefore we can say that in case of diradicals the energy of LUMO decreases sharply due to localization; thus, narrowing the HL gap. We can see here that at high field HOMO is delocalized over whole molecule whereas LUMO is localized on few atoms; i.e., they do not have the same location (Figure 6.5). Another point to be noted from Figure 6.5 is that the HOMO between field strength 0.0115 a.u. and 0.0130 a.u. switches its sign, it indicates changing of symmetry of HOMO with respect to other orbitals. This observation can be explained as the spatial distribution of MO is a function of conformation and external field strength and at 0.0130 a.u. field strength the conformational angle of diradical changes around 10° from the ground state. This may be the reason of change in symmetry of HOMO between field strength 0.0115 a.u. and 0.0130 a.u. The molecules with small HOMO-LUMO gap (band gap) are of potential interest due to their various applicability as in molecular electronics, intrinsic conductor, electrochromic display and charge storage materials.[33] Many researchers have given attention to synthesize the molecules with less HOMO-LUMO gap.[33] Table 6.2 show that the HOMO-LUMO gap reduces with increasing field strength and reaches up to 0.34 eV. Such types of molecules are predicted as unimolecular rectifier.[32] Therefore, the diradical in the field strength beyond 0.0075 a.u. and up to 0.0145 a.u. can be used as unimolecular rectifier. At the field strength 0.0160 a.u. HOMO and LUMO have the same location and have low HL gap which is prerequisite for a molecule to be a molecular conductor.[33] Therefore, at the field strength 0.0160 a.u. it will act as molecular conductor. The change of molecular orbital and hence the current conduction through molecules due to conformational change has been observed by Senapati et al.[3] They also suggest that the conformational changes due to applied electric field may be used as molecular variable resistor

(potentiometer). However, for E⊥ the energy of MO remains more or less unaffected (Appendix 2).

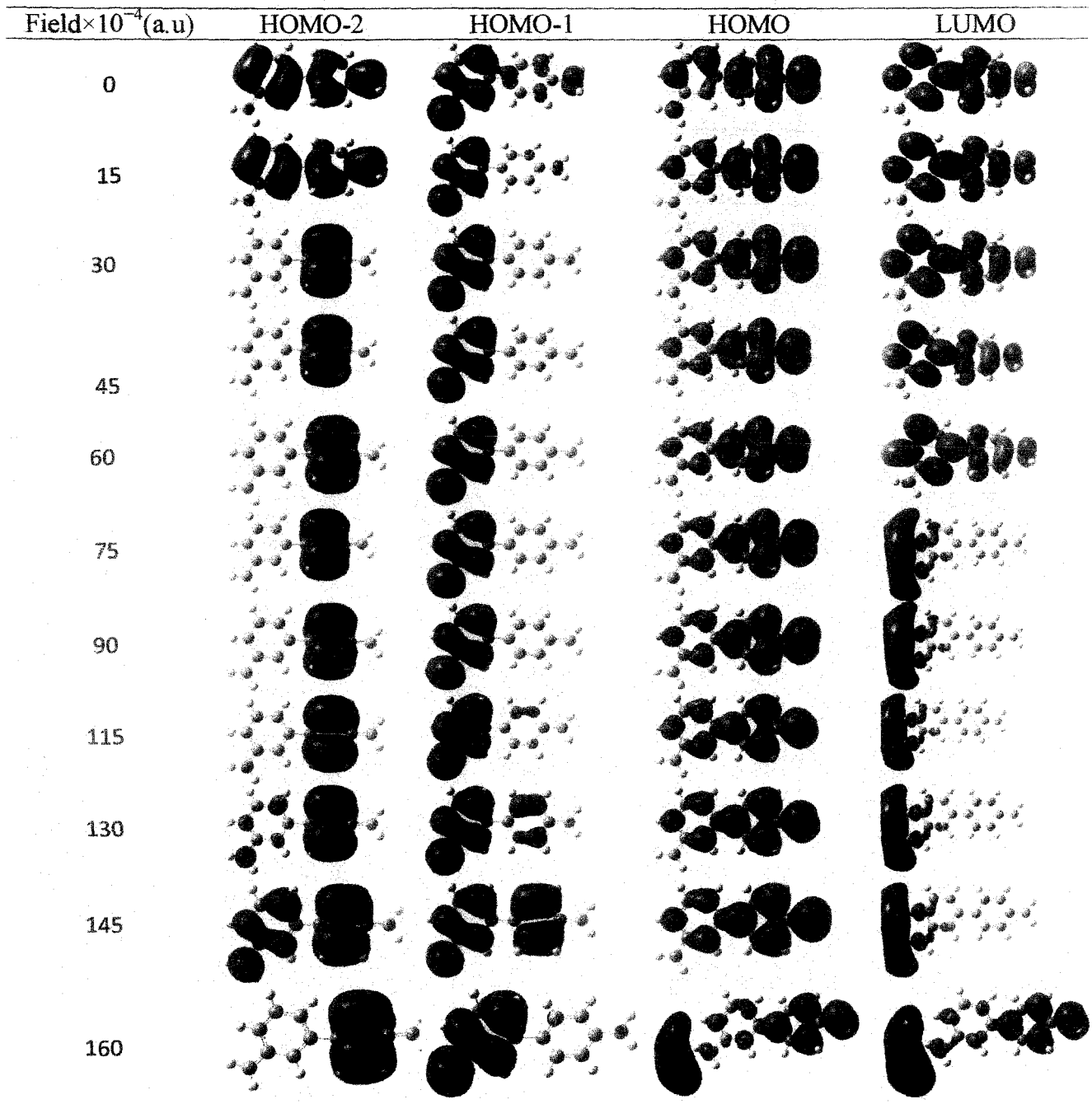

Figure 6.5 The Molecular orbital picture of diradical at various field strength($E_{\parallel}$).

6.2.3 Magnetic exchange coupling constant and spin density of radicals

The above discussion shows that the conformation and molecular orbital energy and spatial distribution are the function of applied external electric field. It is also to be noted that the spin density and magnetic interaction of molecules are largely dependent on the geometry and molecular orbital distribution.[34] Therefore, it is needless to say that the applied electric field will perturb the spin density on the radical centre and magnetic interaction in the diradical. The transport property of radical also depends on the nature of the radical.[35] Keeping these points in mind we have studied the spin density on radical centre and magnetic exchange coupling constant of the diradical under external electric field.

The origin of magnetism in diradical is due to the exchange coupling between radical centers. We have estimated the exchange coupling constant of the diradical under electric field. For the calculation of magnetic exchange coupling constant (J), following our previous works[36] we employ the broken symmetry (BS) Yamaguchi formulae[37] within DFT framework; which is given by

$$J = (E_{BS} - E_T)/\langle S_T^2 \rangle - \langle S_{BS}^2 \rangle \qquad (6.1)$$

In the above, E_{BS} is the energy of the BS state and E_T is that of the triplet state, whereas $\langle S_T^2 \rangle$ and $\langle S_{BS}^2 \rangle$ represent the average spin square values of triplet and BS states respectively. The magnetic interaction in conjugated systems occurs due to the itinerant exchange through π conjugation. We have seen that with increasing field strength ($E_\parallel$) the spin density on radical sites diminishes and increases on the coupler (Figure 6.6). One may anticipate that due to the decrease in spin density on the radical centers the exchange coupling between these two sites should decrease. However, the opposite trend is observed (Table 6.3); i.e., exchange coupling constant increases with field strength ($E_\parallel$). This can be explained in the following way. The dihedral angle (Table 6.1) and C-C bond length between two phenyl rings decreases (bond length changes from 1.48 Å to 1.46 Å) with increasing field strength. Therefore, one can say that the conjugation between two radical centers increases facilitating the itinerant exchange process. As a result, the magnetic exchange coupling constant values of the diradical increase with increasing field strength ($E_\parallel$). With increasing field strength the spin density on the radical centre decreases and increases on the coupler, i.e., the spin density distribution tends to be homogenous in higher

field strength. The spin density is due to π electrons, i.e., the π electrons are distributed over the whole molecule at higher field strength. As a consequence the molecule will show good transport property at higher field and at lower dihedral angle. When the field is applied perpendicular to the molecular plane, the spin density values (Figure 6.6) are less affected by the field. In this situation, the C-C bond length remains unchanged but the dihedral angle increases with increasing field strength (Table 6.3). Consequently the conjugation between two radical centers reduces and hence the exchange coupling constant between two radical centers decreases with increasing field strength ($E_{\perp}$). Thus, lower dihedral angle facilitates the higher exchange coupling between the spins. The larger effect of $E_{\parallel}$ compared to $E_{\perp}$ on spin density can be explained with the help of the shape of polarizable π orbitals. When we apply the electric field parallel (perpendicular) to the molecular plane, the field is actually perpendicular (parallel) to the polarizable π orbitals. A field applied perpendicular to the π orbital has larger effect compared to the parallel one. As a result, the spin density is more affected by $E_{\parallel}$ compared to $E_{\perp}$. In case of mono-radical similar observation of spin density is also scrutinized.

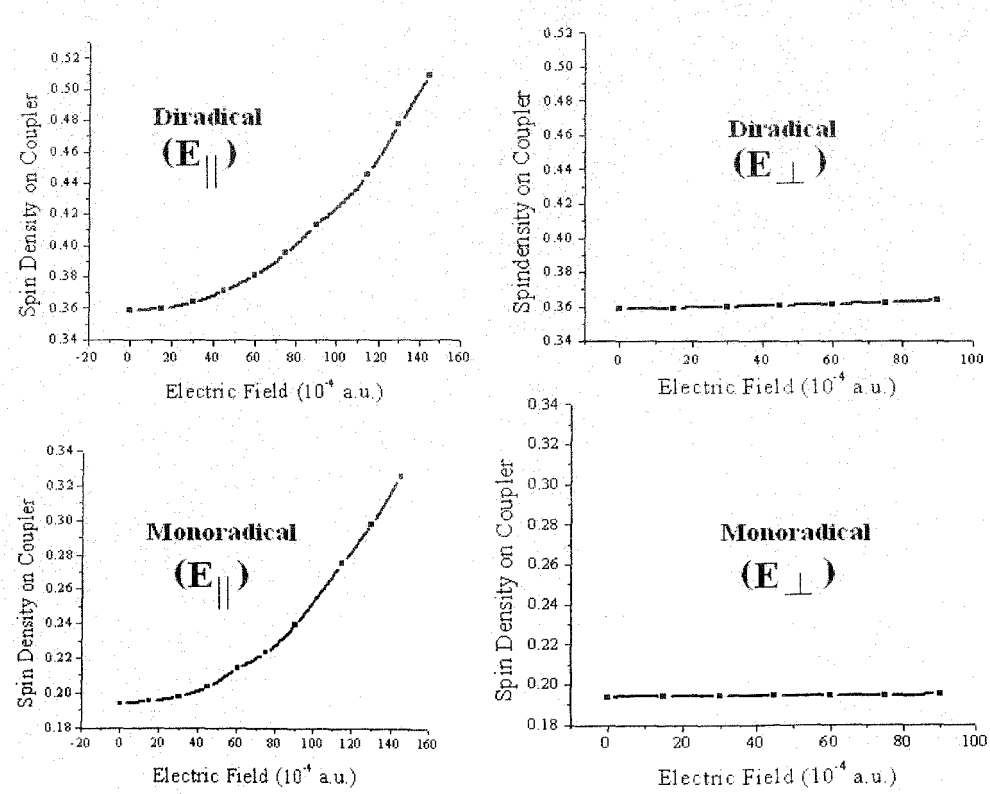

Figure 6.6 Change in spin density on coupler under applied electric field for diradicaland monoradical.

Table 6.3 Energy and Values of Triplet and BS State of the Diradical under Various Electric Field and their Corresponding J Values (1 au field strength = 51.42 V/Å)

Field×10−4 a.u.		$E_{\parallel}$			$E_{\perp}$			
		Triplet	BS	J(cm^{-1})		Triplet	BS	J(cm^{-1})
0	E	−540.68000	−540.67791	449	E	−540.68000	−540.67791	449
	$\langle S^2 \rangle$	2.08	1.05		$\langle S^2 \rangle$	2.08	1.05	
15	E	−540.68029	−540.67820	445	E	−540.68015	−540.67806	447
	$\langle S^2 \rangle$	2.08	1.05		$\langle S^2 \rangle$	2.08	1.05	
30	E	−540.68129	−540.67915	456	E	−540.68054	−540.67846	445
	$\langle S^2 \rangle$	2.08	1.05		$\langle S^2 \rangle$	2.08	1.05	
45	E	−540.68300	−540.68086	469	E	−540.68118	−540.67912	452
	$\langle S^2 \rangle$	2.08	1.05		$\langle S^2 \rangle$	2.08	1.05	
60	E	−540.68545	−540.68314	492	E	−540.68207	−540.68003	436
	$\langle S^2 \rangle$	2.08	1.05		$\langle S^2 \rangle$	2.08	1.05	
75	E	−540.68865	−540.68622	520	E	−540.68321	−540.68121	429
	$\langle S^2 \rangle$	2.08	1.05		$\langle S^2 \rangle$	2.08	1.05	
90	E	−540.69265	−540.69008	546	E	−540.68460	−540.68263	421
	$\langle S^2 \rangle$	2.08	1.04		$\langle S^2 \rangle$	2.08	1.05	

6.2.4 Spin filtering ability of diradical

Organic radicals are promising candidate for the construction of spintronic devices like spin valve, spin filter etc.[35] The molecules with magnetic characteristics has wide applications in the field of spintronics.[38] Therefore organic magnetic molecules are likely to have interesting applicability in this field. Efficient spin filters have appreciably different transmission near Fermi level.[35] We have calculated the transmission spectra of diradicals at different dihedral angles to understand the spin filtering ability of diradicals with respect to their dihedral angle as we have discussed earlier. The diradical molecule is placed between two Au electrodes in a two-probe transport structure, as shown in Figure 6.7.

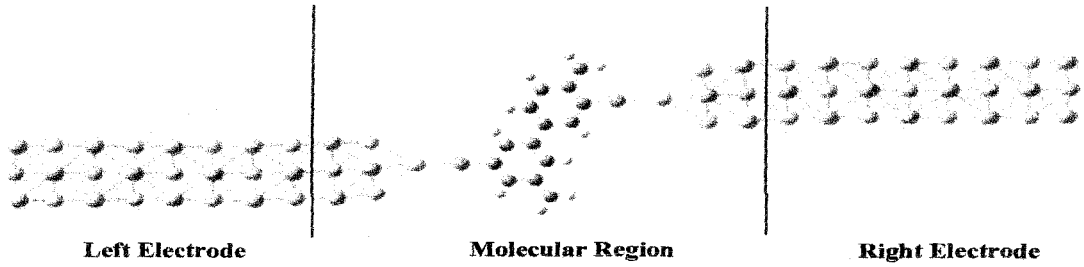

Figure 6.7 The Au-diradical-Au two-probe transport structure. Semi-infinite leads extending to ∞ (left and right boxes) are bridged by the diradical molecule in the molecular region (center box).

The electrodes are modeled as nano wires with 3 × 3 cross section in the (100) direction. At the end of each electrode, there is an Au adatom that connects with S atoms. Then the electrodes are extended into quasi-one-dimensional leads by adding Au atoms at their appropriate bulk lattice positions in a 3 × 3 wire extending in the (100) direction which leads to the structure shown in Figure 6.7. This is the two-probe structure on which the transport calculations have been performed. It consists of three parts; a left lead, a molecular region, and a right lead (see Fig. 9). Each lead is semi-infinite, extending to z direction while the molecular region contains a portion of each lead and the diradical molecule. We use PBE functional and SZP basis set for the transmission calculation. The transmission calculation has been done using Transiesta programme package.[39] The transmission is obtained from the equation

$$T(E) = Tr\left[\Gamma_L(\varepsilon)G^{\dagger}(\varepsilon)\Gamma_R(\varepsilon)G(\varepsilon)\right] \tag{6.2}$$

where $\Gamma_L(\varepsilon)$ and $\Gamma_R(\varepsilon)$ are the self energies of left and right electrode, $G^{\dagger}(\varepsilon)$ and $G(\varepsilon)$ are the retarded and advanced Green's function.

In the nonequilibrium Green's-function formalism the current I through the contact can be derived as

$$I(V) = G_0 \int_{-\infty}^{\infty} d\varepsilon \left[n_F(\varepsilon - \mu_L) - n_F(\varepsilon - \mu_R)\right] \times T(E) \tag{6.3}$$

where $G_0=2e^2/h$, μ_L and μ_R are the chemical potentials of left and right electrodes respectively.

The calculated transmission spectra and spin current at 0V and 1V is presented in Figure 6.8. We can see from Figure 6.8 that at 0V maximum transmission comes out at equilibrium ground state geometry and it gradually decreases with decreasing dihedral angle. On the other hand, at 1V the transmission spectrum shows opposite trend. The separation between alpha and beta transmission suggests about the spin filtering ability of a molecule. We can see that when the dihedral angle of the diradical is low (21°), the transmission of alpha and beta electrons differ by a broad energy range, which is a prerequisite for a molecule to show efficient spin filtering ability. Therefore we can say that it can act as an efficient spin filter in this conformation. We have also calculated the current (I) at 1V to examine the spin filtering efficiency at different dihedral angles. It is seen that at ground state geometry the up and down spins have comparable current (I_{UP}= 0.30 nA I_{Down}= 0.50 nA), with decreasing dihedral angle the up spin current conduction decreases whereas down spin current conduction increases (Figure 6.9). Therefore, we can suggest that at lower dihedral angle the diradical acts as an efficient spin filter. That is, after setting up the molecular device, if one applies appropriate external electric field the device will behave as efficient spin filter at lower dihedral angle as dihedral angle decreases upon application of external electric field.

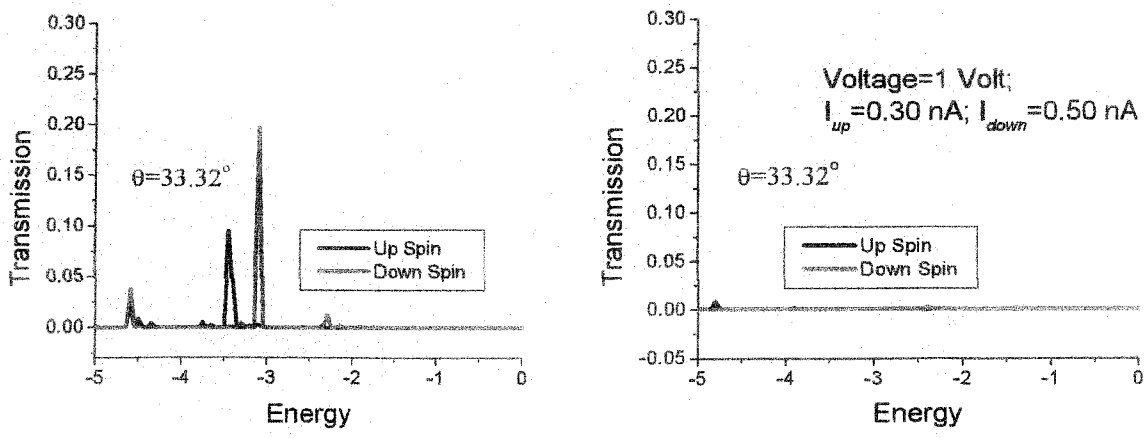

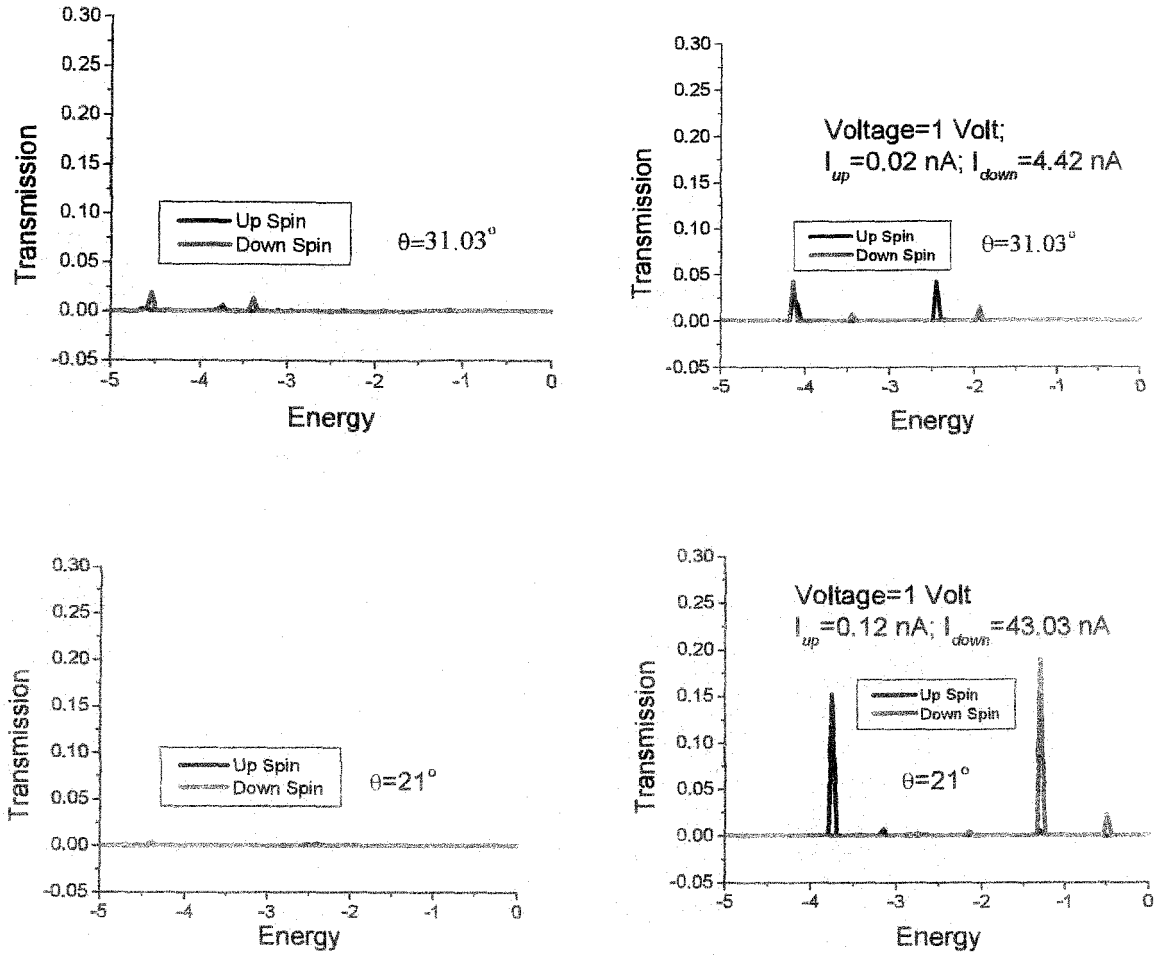

Figure 6.8 Transmission spectra (Black and red colour represents the up and down electron transmission respectevely) of diradical at various dihedral angle and the spin current.

6.2.5 Current–Voltage (I-V) curves

Figure 6.9 depicts the *I-V* curves for the diradical at different dihedral angles. The black line represents the up spin current, red line represents the down spin current and green line represents the total current carried by up and down spins. We have seen here that at ground state geometry (dihedral angle 33.32°) the current conduction increases after the threshold voltage 1.5V whereas for dihedral angle 21° the threshold voltage is 0.5V. The strength of current conduction by one spin component is much greater than the other in case of the dihedral angle 21° compared to other dihedral angles. This observation tells us that when one spin actively

conducts current, other spin remains inactive. This is also understandable from transmission spectra which is depicted in Figure 6.8 where the sufficient energy difference between up and down spin transmission is observed in 21° dihedral angle. Therefore, we can say that at lower dihedral angle the diradical has higher conductivity and spin filtering ability. To ensure the spin filtering ability of the diradical at 21° dihedral angle, we quantify spin polarization at finite bias in terms of spin-resolved currents[40]

$$I_S = \frac{I_{up} - I_{down}}{I_{up} + I_{down}} \tag{6.4}$$

where I_{up} and I_{Down} represent up and down spin currents respectively. We have found that the diradical at 21° dihedral angle has sufficient spin filtering ability (Figure 6.9). We get upto 99% spin filtering efficiency between bias voltage 1V and 1.5V (Figure 6.10).

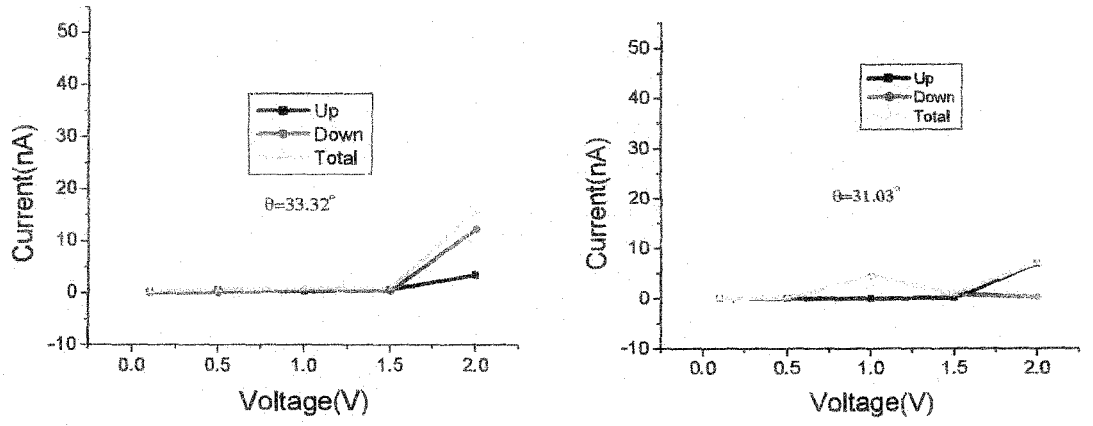

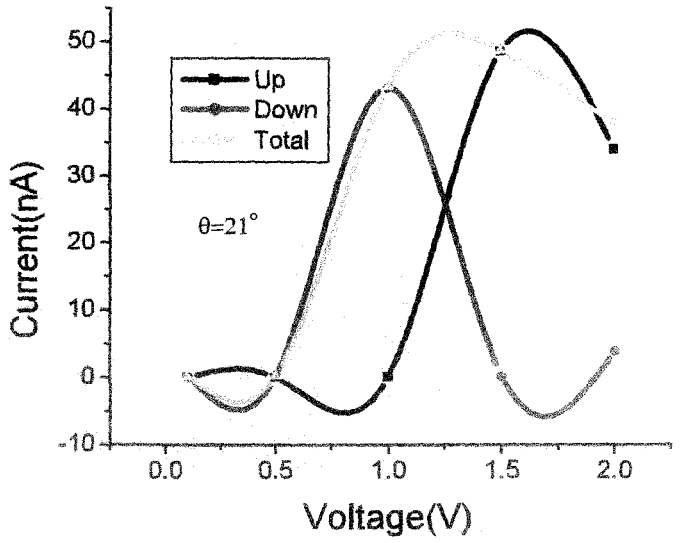

Figure 6.9 Current vs Voltage (*I-V*) curve of the diradical at different dihedral angle.

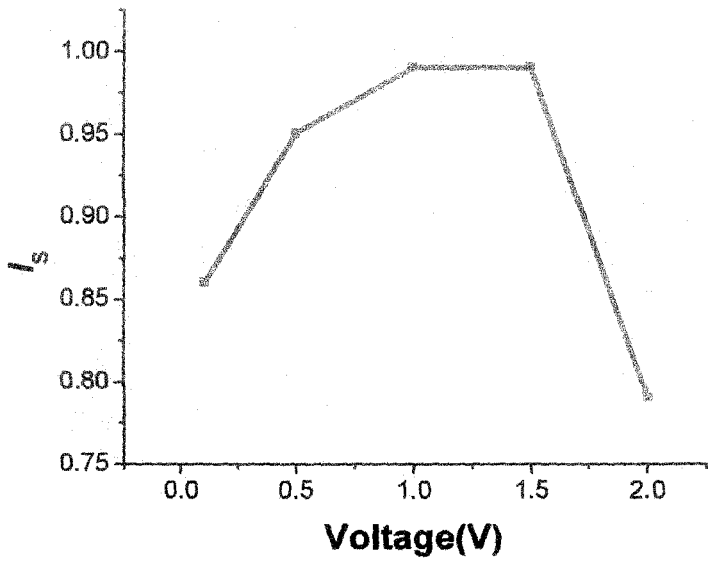

Figure 6.10 I_S vs Voltage (I_S-V) curve of the diradical at 21° dihedral angle.

6.3 Conclusions

To summarize, we study the effect of external electric field on biphenyl, methylene substituted biphenyl mono- and di-radicals. We apply electric field parallel to the molecule ($E_{\parallel}$) and perpendicular to the molecular plane ($E_{\perp}$). It has been observed that one can reversibly tune the molecular conformation by external electric field. This result provides an alternative way to change the molecular conformation without any chemical substitution; i.e, tuning of molecular conformation by external means. The energy and spatial distribution of molecular orbital are found to be the function of external electric field. Among these systems, the low HL gap has been achieved in case of diradical by application of external elctric field. This low HL gap has wide applicability in the field of molecular electronics. It has been found that the diradical in the field strength between 0.0075 a.u. and 0.0145 a.u. can be used as unimolecular rectifier. At the field strength 0.0160 a.u. it can act as molecular conductor. The spin density distribution of the monoradical and diradical are dependent on the strength and direction of the external electric field. It has been found that $E_{\parallel}$ has more effect on spin density than $E_{\perp}$. With increasing field strength the spin density on radical centre decreases and increases on the coupler. The lower dihedral angle fascilitates the higher conjugation between the spins in diradical resulting the increase in magnetic exchange coupling constant. Therefore, one can tune the strength of magnetic exchange coupling constant by external electric field. With increasing the magnetic exchange coupling constant current conduction of the diradical also increases. There is appreaciable difference of up spin and down spin transmission spectra at lower dihedral angle. This observation confirms the spin filtering ability of the diradical at lower dihedral angle. It is seen that at ground state geometry of the diradical the up and down spins conduct comparable current. While, with decreasing dihedral angle the up spin current conduction decreases, on the other hand down spin current conduction increases. That is, at lower dihedral angle the diradical acts as an efficient spin filter. We have found that the diradical at 21° dihedral angle has 99% spin filtering efficiency between bias voltage 1V and 1.5V. Therefore, a single molecule can be used for different appication like unimolecular rectifier, spin filter and molecular conductor varying the strenght of the external electric field.

6.4 References

1. Heath, J. R.; Ratner, M. A. *Phys. Today* **2003**, *56*, 43.
2. Dutta, A.; Pati, S. K. *Chem. Soc. Rev.* **2006**, *35*, 1305.
3. Senapati, L.; Pati, R.; Erwin, S. C. *Phys. Rev. B* **2007**, *76*, 024438.
4. Mckinney, J. D.; Singh, P. *Chem.-Biol. Interact.* **1981**, *33*, 271.
5. Pancir, J.; Zahradnik, R. *Helv. Chim. Acta* **1978**, ***61***, 59.
6. Pancir, J.; Haslingerova, I. *Collect. Czech. Chem. Commun.* **1980**, *45*, 2474.
7. Rai, D.; Joshi, H.; Kulkarni, A. D.; Gejji, S. P.; Pathak, R. K. *J. Phys. Chem. A* **2007**, *111*, 9111.
8. Li, Y.; Zhao, J.; Yin, X.; Yin, G. *J. Phys. Chem. A* **2006**, *110*, 11130.
9. Wang, C. K.; Fu, Y.; Luo, Y. *Phys. Chem. Chem. Phys.* **2001**, *3*, 5017.
10. Tóbik, J.; Corso, A. D.; Scandolo, S.; Tosatti, E. *Surf. Sci.* **2004**, *566*, 644.
11. Manuel Smeu, M.; DiLabio, G. A. *J. Phys. Chem. C* **2010**, *114*, 17874.
12. Tagami, K.; Tsukada, M. *J. Phys. Chem. B* **2004**, *108*, 6441.
13. Tao, N. J. *Nat. Nanotechnol.* **2006**, ***1***, 173.
14. Trotter, J. *Acta Cryst.* **1961**, *14*, 1135.
15. Hargreaves, A.; Rizvi, S. H. *Acta Cryst.* **1962**, *15*, 365.
16. Robertson, G. B. *Nature* **1961**, *191*, 593.
17. Bastiansen, O. *Acta Chem. Scand.* **1950**, *4*, 926.
18. Johansson, M. P.; Olsen, J. *J. Chem. Theory Comput.* **2008**, *4*, 1460.
19. Bastiansen, O.; Samdal, S. *J. Mol. Struct.* **1985**, *128*, 115.
20. Stroh, C.; Mayor, M.; von Hänisch, C. *Eur. J. Org. Chem.* **2005**, 3697.
21. Mostovich, E. A.; Borozdina, Y.; Enkellmann, V.; Remović-Langer, K.; Wolf, B.; Lang, M.; Baumgarten, M. *Cryst. Growth Des.* **2012**, *12*, 54.
22. Frisch, M. J. et al., Gaussian 09, revision B.01; Gaussian, Inc.: Wallingford, CT, 2010.
23. Szymoszek, A.; Koll, A. *Chem. Phys. Lett.* **2003**, *373*, 591.
24. (a) Oliveira, F. A. C.; Cury, L. A.; Righi, A.; Moreira, R. L.; Guimaraes, P. S. S.; Matinaga, F. M.; Pimenta, M. A.; Nogueira, R. A. *J. Chem. Phys.* **2003**, *119*, 9777. (b) Cornil, J.; Beljonne, D.; dos Santos, D. A.; Shuai, Z.; Bre´das, J. L. *Synth. Met.* **1996**, *78*, 209.

25. Casado, J.; Hicks, R. G.; Hernandez, V.; Myles, D. J. T.; Ruiz Delgado, M. C.; Lopez-Navarrete, J. T. *J. Chem. Phys.* **2003**, *118*, 1912.

26. Weiss, E. A.; Tauber, M. J.; Kelley, R. F.; Ahrens, M. J.; Ratner, M. A.; Wasielweski, M. R. *J. Am. Chem. Soc.* **2005**, *127*, 11842.

27. Li, Y.; Zhao, J.; Yin, X.; Liu, H.; Yin, G. *Phys. Chem. Chem. Phys.* **2007**, *9*, 1186.

28. Kim, W. Y.; Kim, K. S. *Acc. Chem. Res.* **2010**, *43*, 111.

29. Choi, Y. C.; Kim, W. Y.; Park, K. –S.; Tarakeshwar, P.; Kim, K. S. *J. Chem. Phys.* **2005**, *122*, 094706.

30. Tour, J. M.; Kozaki, M.; Seminario, J. M. *J. Am. Chem. Soc.* **1998**, *120*, 8486.

31. Kairys, V.; Head, J. D. J. *Phys. Chem. A* **1998**, *102,* 1365.

32. Aviram, A.; Ratner, M. A. *Chem. Phys. Lett.* **1974**, *29*, 277.

33. Perepichka, D. F.; Bryce, M. *Angew Chem. Int. Ed.* **2005**, *44*, 5370 and references therein.

34. Shil, S.; Paul, S.; Misra, A. *J. Phys. Chem. C* **2013**, *117*, 2016.

35. Herrmann, C.; Solomon, G. C.; Ratner, M. A. *J. Am. Chem. Soc.* **2010**, *132*, 3682.

36. (a) Bhattacharya, D.; Misra, A. *J. Phys. Chem. A* **2009**, *113*, 5470. (b) Paul, S.; Misra, A. *J. Mol. Str. (THEOCHEM)* **2009**, *907*, 35. (c) Paul, S.; Misra, A. *J. Mol. Str. (THEOCHEM)* **2009**, *156*, 895. (d) Bhattacharya, D.; Shil, S.; Panda, A.; Misra, A. *J. Phys. Chem. A* **2010**, *114*, 11833. (e) Paul, S.; Misra, A. *J. Phys. Chem. A* **2010**, *114*, 6641. (f) Bhattacharya, D.; Shil, S.; Misra, A.; Klein, D. J. *Theor. Chem. Acc.* **2010**, *127*, 57. (g) Paul, S.; Misra, A. *J. Chem. Theor. Comput.* **2012**, *8*, 843.

37. (a) Yamaguchi, K.; Takahara, Y.; Fueno, T.; Nasu, K. *Jpn. J. Appl. Phys.* **1987**, *26*, L1362. (b) Yamaguchi, K.; Jensen, F.; Dorigo, A.; Houk, K. N. *Chem. Phys. Lett.* **1988**,*149*, 537. (c) Yamaguchi, K.; Takahara, Y.; Fueno, T.; Houk, K. N. *Theor. Chim. Acta.* **1988**, *73*, 337.

38. Aravena, D.; Ruiz, E. *J. Am. Chem. Soc.* **2012**, *134*, 777.

39. Brandbyge, M.; Mozos, J.-L.; Ordejon, P.; Taylor, J.; Stokbro, K. *Phys. Rev. B* **2002**, *65*, 165401.

40. Parida, P.; Basheer, E. A.; Pati, S. K. *J. Mater. Chem.* **2012**, *22*, 14916.